

Comprehensive Data of a Grain Oriented Reference Material for Efficient Modelling of Axial Flux Machines

Downloaded from: https://research.chalmers.se, 2026-11-08 10:45 UTC

Citation for the original published paper (version of record):
Puttaraj, V., Tidblad Lundmark, S., Thiringer, T. (2026). Comprehensive Data of a Grain Oriented Reference Material for Efficient Modelling of Axial Flux
Machines. 2026 International Conference on Electrical Machines (ICEM).
http://dx.doi.org/10.1109/ICEM68283.2026.11757092

N.B. When citing this work, cite the original published paper.

research.chalmers.se offers the possibility of retrieving research publications produced at Chalmers University of Technology. It covers all kind of research output: articles, dissertations, conference papers, reports etc. since 2004. research.chalmers.se is administrated and maintained by Chalmers Library

(article starts on next page)

Comprehensive Data of a Grain Oriented Reference Material for Efficient Modelling of Axial Flux Machines

Vineetha Puttaraj
Department of Electrical Engineering
Chalmers University of Technology
Gothenburg, Sweden
vineetha@chalmers.se or

Sonja Tidblad Lundmark
Department of Electrical Engineering
Chalmers University of Technology
Gothenburg, Sweden
sonja.lundmark@chalmers.se or

Torbjörn Thiringer
Department of Electrical Engineering
Chalmers University of Technology
Gothenburg, Sweden
torbjorn.thiringer@chalmers.se or

2026 International Conference on Electrical Machines (ICEM) | 979-8-3315-6232-8/26/$31.00 ©2026 IEEE | DOI: 10.1109/ICEM68283.2026.11757092

***Abstract*—This paper focuses on Grain-Oriented Electrical Steel (GOES) for rotating electrical machines, specifically the Yokeless And Segmented Armature (YASA) type Axial Flux Machine (AFM). Accurate modelling of GOES is essential for a reliable loss prediction in rotating electrical machine simulations. However, complete flux measurement in different directions is often unavailable for many GOES. This work presents a practical approach to estimate the core loss in different flux directions for a research GOES material using limited available material data. The B-H and B-P curves of three reference materials with known data in the Rolling Direction (RD) and some data in the Transverse Direction (TD) were analysed to understand the relationship between core loss in different flux directions. Based on this comparison, research material data was constructed using a simple scaling approach. The researched GOES material was used in YASA AFM and it was found that the average core loss is reduced by 28% compared to a Non-Oriented (NO) stator core.**

***Index Terms*—Axial Flux Machines, YASA AFM, Electrical Steel, Isotropic Material, Anisotropic Material, Grain Oriented Electrical Steel, Non Oriented Electrical Steel.**

I. Introduction

THE performance of the electric machine largely depends on the materials used and their associated properties. The selection of suitable traction drive motors involves certain criteria, such as a higher torque-to-weight ratio, sustainability, and manufacturability. The Axial Flux Machine (AFM) topology is becoming attractive due to its possibility of higher torque-to-weight ratio compared to a Radial Flux Machine (RFM).

The selection of electrical steel for the core material significantly affects the achievable flux density, losses, and saturation [1], [2]. The Non-Oriented Electrical Steel (NOES) and Grain-Oriented Electrical Steel (GOES) are the two widely used electrical steel materials in electrical machines. The magnetic properties of NOES are more uniform in all directions; this property makes them more commonly used in motors and generators. However, GOES has aligned grain structures oriented along the Rolling Direction (RD) of the steel. This alignment enhances magnetic performance in the RD, making it ideal for cores where magnetic flux flows predominantly in one direction.

The GOES is generally avoided in the RFMs because the flux paths in the teeth and yoke are perpendicular. If flux in tooth would go along the RD, the flux in the yoke would go along the Transverse Direction (TD). In addition, the teeth are curved or arched near the air gap. This curvature causes the local magnetic flux vector to continuously change direction along the tooth length. In contrast, AFM employs more planar teeth in which the magnetic flux remains largely in a single in-plane direction, even when trapezoidal tapering is present.

In [3], magnetic analysis was performed to apply GOES to traction motors. The tooth material is changed to perform a performance comparison under equivalent current conditions, showing that GOES shows superior iron loss density characteristics at lower frequencies.

In [4], a novel type of permanent magnet-assisted synchronous reluctance motor was proposed, where GOES was used for the stator teeth. The results showed an increase of 12% torque and a decrease of 11% in iron loss under the no-load conditions.

In [5], a Yokeless And Segmented Armature (YASA) AFM was analyzed with GOES, NOES, Soft Magnetic Composites (SMC), and amorphous alloy for the yoke. The results showed that GOES as the stator core material can maximize the output torque, the amplitude of the no-load back-emf, and the inductance of the YASA AFM, choosing SMC can minimize the harmonic distortion of the no-load back-emf and the torque ripple, and choosing amorphous alloy can maximize the efficiency of the YASA AFM.

A Double Stator Single Rotor (DSSR) type AFM with GOES stator teeth is analysed in [6]. The teeth geometry was redesigned by optimizing the dimensions of the slot, tooth, and pole. It was demonstrated that, compared to a core with NOES, the teeth with GOES increased in torque by 4%, and the optimized geometry had an increase of 10% in torque. Iron losses in both situations with GOES material were reduced by 14%.

In [7], a Grain-Oriented (GO) silicon steel in YASA type

The authors gratefully acknowledge the financial support provided by the Swedish Electromobility Center and K.G.Hallby's fund.

Authorized licensed use limited to: Chalmers University of Technology Sweden. Downloaded on November 05,2026 at 14:27:58 UTC from IEEE Xplore. Restrictions apply.

AFM is employed to improve the torque and efficiency. However, the author states that dividing the stator into teeth and yoke to achieve different lamination directions will result in a low structural strength of the machine and a complex manufacturing process.

In [8], the performance and iron losses of an Axial Flux Permanent Magnet (AFPM) machine for a Single Stator Double Rotor (SSDR) type with NOES and GOES were compared. It was identified that the chosen GOES material had around 7 times lower iron loss at the same speed compared to NOES, and a 10% higher torque for the same current.

When calculating core loss, it should be considered that core loss is influenced not only by the time and space discretisation of the used numerical method and by the quality of the used material data, but core loss is also affected by manufacturing processes and harmonic effects. As shown in [9], core losses increase as a result of cutting processes, where the relative rise in core losses is reported to be approximately 120–180% for laser cutting, 40–50% for punching, and around 6% for waterjet cutting.

To perform comparisons of torque and loss, as described above, accurate data is needed, and this is often lacking regarding the GOES, especially for the TD, and at frequencies above 60 Hz. The main contribution of this work is the description of how to perform electromagnetic analysis of the complicated AFM with anisotropic core materials. Where, more specifically, a GOES research material is suggested, where all the needed data is given such as the magnetization characteristics and core loss data for both the TD and the RD, and for different frequencies. Data found from data sheets [10] and references [11] and [7] are used as a base. Cutting effects are not considered in this work and core loss coefficients (K_h, K_c, K_e) are extracted using Ansys Maxwell's material characterization tool by fitting multifrequency $B-P$ curves to the Bertotti loss separation model [12].

II. Magnetic Anisotropy in Electrical Steel

A. B–H characteristics in rolling vs transverse direction

GO (anisotropic) steel has grains aligned along the RD, resulting in a steep B-H curve, with high permeability, and a narrow hysteresis loop along this direction, but with worse magnetic properties perpendicular to it. In contrast, Non-Oriented (NO) (isotropic) steel has randomly oriented grains, producing a more uniform but moderate B-H response in all the directions, with lower peak flux density and higher losses.

In GOES, the magnetic properties like permeability and saturation vary significantly depending on the direction of the applied field [13]. When a rotating magnetic field interacts with such material, the flux does not rotate uniformly; instead, it tends to snap towards the material's RD, leading to distorted field shapes. However, these effects are typically seen as a disadvantage in standard motor topologies where the field must sweep across the steel.

In a YASA AFM, the impact of anisotropy is unique due to its segmented stator geometry. Unlike traditional motors where the magnetic field rotates through a continuous yoke, the YASA AFM design isolates the flux within an individual axial tooth. This allows the GOES to be aligned so that the flux remains primarily linear and alternating along its preferred RD, effectively bypassing the complexities of a truly rotating field within the core itself. Consequently, this work focuses on how the YASA AFM architecture leverages these directional properties by reducing the losses.

B. Limitations in Available Directional Core-Loss Data

Accurate prediction of core losses in rotating electrical machines depends on knowing the material's directional loss characteristics. For GOES, losses are highly anisotropic: magnetization along the RD produces significantly lower losses than along the TD. Despite the importance, experimental data for off-axis and rotational magnetization is extremely limited. The absence of such data poses several problems like inaccurate loss estimation, design optimization challenges, and simulation uncertainty.

III. Yokeless And Segmented Armature (YASA) AFPM Modelling Approach

An off-the-shelf inner rotor outer stator machine in [14] was used as the benchmark machine to model the YASA AFM. The motor ratings and dimensions are similar to the reference machine from [14]. The equivalent YASA machine is built with Finite Element Method (FEM) modelling in ANSYS Maxwell software. The machine data, like rated power, rated torque, and speed with dimension details, are presented in Table I.

TABLE I
YASA AFPM machine data

Description	Value
General details	
Rated power	4 kW
Peak power	8 kW
Rated speed	2000 rpm
Maximum speed	4000 rpm
Rated torque	19 Nm
Peak Torque	50 Nm
Number of poles	16
Number of slots	18
Type of cooling	Natural air cooling
Dimension details of reference machine and 3D model	
Outer diameter of stator core	166.2 mm
Inner diameter of stator core	94.2 mm
Outer diameter of rotor core	166.2 mm
Inner diameter of rotor core	38 mm
Length of magnet in radial direction, L_m	34 mm
Length of tooth in radial direction	36 mm
Stator core length in positive z-direction	30 mm
Total rotor core and magnet length in z-direction	7 mm
Winding details	
Diameter of single copper strand	0.88 mm
Number of winding layers	2
Number of turns	10
Number of parallel branches	1
Type of winding	Concentrated

The YASA AFM 3D model presented in Fig. 1, consists of an inner yokeless stator, and two outer rotors with surface PMs. The rotor yoke is assigned with a magnetically leading material so it completes the flux path. However, solving 3D

Authorized licensed use limited to: Chalmers University of Technology Sweden. Downloaded on November 05,2026 at 14:27:58 UTC from IEEE Xplore. Restrictions apply.

models is time-consuming, hence the 3D model is transformed to a 2D model, and the transformation process involved is illustrated in Fig. 2. In the rest of the work, the 2D model of the machine will be used for further analysis of the core loss. The stator core material was represented as a solid (rather than a lamination with a set stacking factor, k_{FE}). This was done to reduce computational complexity, while still capturing the main electromagnetic behaviour, but also since some inconsistencies were found from the 3D FEM solutions with a stacking factor (not getting the same result with a solid material as with a lamination with a stacking factor, $k_{FE} = 1$). The stator core was thus modelled as a solid with zero conductivity, thus representing a homogenized laminated material that does not consider detailed inter-laminar eddy current effects. When two sliding bands were initially

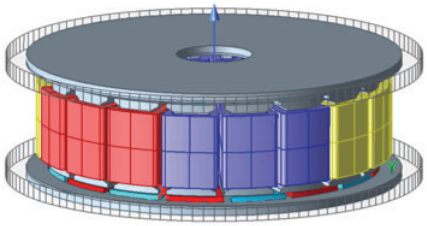


Fig. 1. 3D YASA AFM model

applied (one for each rotor), the predicted torque became almost twice the expected value, despite refining the mesh and using smaller time steps. The flux linkage and induced voltage did not change, which indicates that the difference was not due to the magnetic solution itself, but due to how the torque from the two identical air gaps is being accounted for in the post-processing. Using a single sliding band around the stator avoids this double-counting.

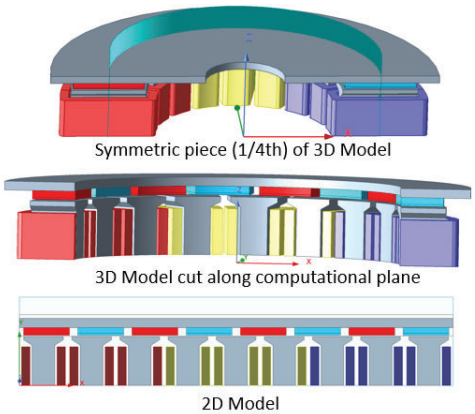


Fig. 2. Illustration of transforming 3D to 2D model

IV. Grain-Oriented Electrical Steel (GOES) Material Characterization

Modelling anisotropy for a GOES requires B-H curves in both RD and TD. The initial process of modelling involves figuring out the material coordinates, namely RD, TD, and stacking direction. For the 3D stator single segment, the material coordinates are illustrated in Fig. 3. In the transformed 2D model, the GOES material coordinates are: TD in *x-axis*, RD in *y-axis*, and stacking direction in *z-axis*, respectively.

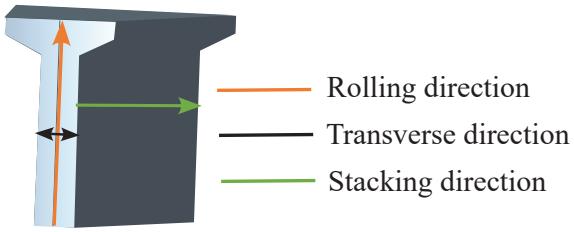


Fig. 3. Material coordinate system for 3D model of top half of stator teeth

Magnetic anisotropy is a well known characteristic of electrical steel arising from the rolling process during manufacturing. As a result, the magnetic behaviour along the RD and TD differs significantly, particularly in the non linear and saturation regions of the magnetization curve. However, in practical material characterization, complete directional measurements are often unavailable, and the manufacturers typically provide the magnetic data mainly along the RD. This limitation poses challenges when accurate anisotropic material properties are required for the FEM model simulations.

To address this issue, a data-driven anisotropic interpolation methodology is proposed to estimate the TD magnetization characteristics using the available data for selected materials used in the rotating electrical machines. The chosen GOES are 20QG085 [7] (with a lamination thickness, $\delta_{th} = 0.2mm$), 35ZH135 [11] ($\delta_{th} = 0.35mm$) and ARMCO M-6 steel [10] ($\delta_{th} = 0.35mm$) for directional scaling framework. The B-H curves in RD and TD are presented in Fig. 4.

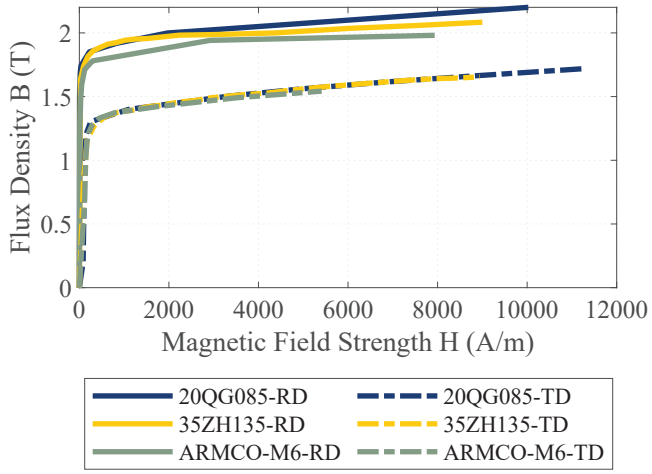


Fig. 4. *B-H* curve for selected material from references

The approach first exploits the ratio between the RD and TD magnetic responses through a flux density-dependent anisotropy factor, which describes how hard it is to magnetize the material in the TD compared to the RD, and this difference changes depending on the flux density level. For the same magnetic flux density **B**, a higher magnetic field **H** is required in the TD than in the RD. The ratio between these two

Authorized licensed use limited to: Chalmers University of Technology Sweden. Downloaded on November 05,2026 at 14:27:58 UTC from IEEE Xplore. Restrictions apply.

field strengths can be described using an anisotropy factor. Since the difference between the two directions changes as the material moves from the linear region to the saturation region, this factor is considered to be dependent on the flux density. Subsequently, the obtained TD data are represented using a model that captures the three characteristic magnetization regions of the magnetic materials, namely the linear, knee, and saturation regions. This formulation provides a smooth and computationally efficient representation of the TD magnetization curve, making it suitable for numerical implementation in electromagnetic simulations while preserving the essential anisotropic behaviour of the material.

The relationship between magnetic field strength **H** in A/m and magnetic flux density **B** in T is described by the constitutive relation

$$\mathbf{B} = \mu \mathbf{H} \tag{1}$$

where μ is the magnetic permeability, which is not a constant for electrical steel and hence the relationship becomes non linear. The *B-H* curve in Fig. 4 is split into three regions.

- Region 1 is linear approximation, termed as linear region, it is defined at low magnetic fields where the magnetic domains align easily and permeability is almost constant.
- Region 2 is the knee region, as **B** increases, the domain rotations becomes harder and the permeability decreases and the curve become non-linear. A smooth non-linear function is required in this region.
- Region 3 is the saturation region where the curve becomes almost linear again but with a very steep slope.

The low-field region of the B-H curve was approximated as linear to ensure numerical robustness and stable convergence in ANSYS Maxwell, since the initial S-shaped toe region may cause interpolation sensitivity and solver instability. As the investigated AFM operates mainly near rated flux density, beyond this low-field region, the impact of this simplification on the main electromagnetic quantities and total core-loss prediction is limited.

The split in the *B-H* curve needs two transition points which defines the region boundaries. The two transition points are B_1 marking the end of linear region 1 and B_2 marking the start of linear region 3. For the knee region, region 2, we need a function that starts at (B_1, H_1) and ends at (B_2, H_2), when the flux density is normalized and a polynomial growth equation is utilized,

$$H_{TD}(B) = H_1 + (H_2 - H_1)\left(\frac{B - B_1}{B_2 - B_1}\right)^n \tag{2}$$

The exponent n controls the curvature in the knee region and the most approximate range is $2 \leq n \leq 4$. After B_2, the curve becomes approximately linear again ensuring continuity at B_2, and the saturation region is modelled as a linear extension beyond B_2 with a slope $k_{sat} = dH/dB$ representing the low incremental permeability of the material in high-flux density conditions,

$$H_{TD}(B) = H_2 + k_{sat}(B - B_2) \tag{3}$$

The final piecewise equation combining three regions is represented as

$$H_{\mathrm{TD}}(B) = \begin{cases} \dfrac{H_1}{B_1} B, & B \leq B_1 \\ H_1 + (H_2 - H_1)\left(\dfrac{B - B_1}{B_2 - B_1}\right)^n, & B_1 < B \leq B_2 \\ H_2 + k_{\mathrm{sat}}(B - B_2), & B > B_2 \end{cases} \tag{4}$$

The derived B-H in the TD for the research material is presented in Fig. 5. It is based on the B-H in the RD from [15], using the proposed method in (4), with the values of the B-H in the RD and TD, B_1, B_2, n, and K_{sat} given in the Appendix.

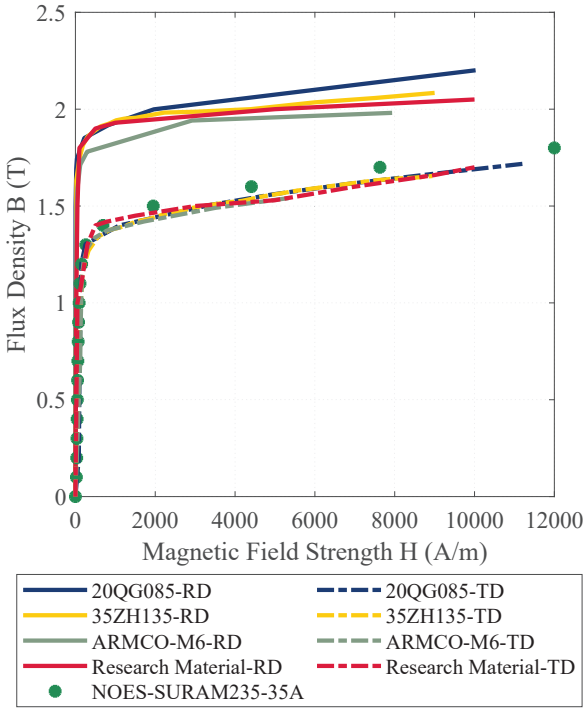


Fig. 5. *B-H* curve in RD and TD from the proposed method

V. Directional Core-Loss Behavior and Sensitivity Analysis in Grain-Oriented Steel

The magnetic properties and core losses depend on the direction of magnetization relative to RD of the laminations. Magnetization along RD produces the lowest core loss, while magnetizations along TD results in significantly higher losses.

A. Representation of B-P Curve

Often, the available B-P curve represents the specific loss as a function of flux density and frequency under RD excitation, and only at a few specific frequencies (for example $50Hz$, $100Hz$, $200Hz$). However, it is important to recognize that the measured B-P curve corresponds strictly to the condition $\theta = 0°$, where θ represents the angle between the magnetization vector and RD. In YASA AFM the magnetic flux within the stator laminations does not remain aligned with this direction. Instead, the flux vector evolves spatially and temporally, producing magnetization states that deviate from

Authorized licensed use limited to: Chalmers University of Technology Sweden. Downloaded on November 05,2026 at 14:27:58 UTC from IEEE Xplore. Restrictions apply.

RD and may approach the rotational excitation partially. Under such conditions, the effective loss is generally described as,

$$P = P\left(B, f, \theta\right) \tag{5}$$

This highlights the directional dependence of core loss in anisotropic materials. The manufacturer data rarely include measurements for arbitrary magnetization angles, the RD B-P curve serves as the baseline representation of the material's loss behaviour.

In this study, B-P curves from [11], [7], and [10], as seen in Fig. 6, are used as the base curves. The research

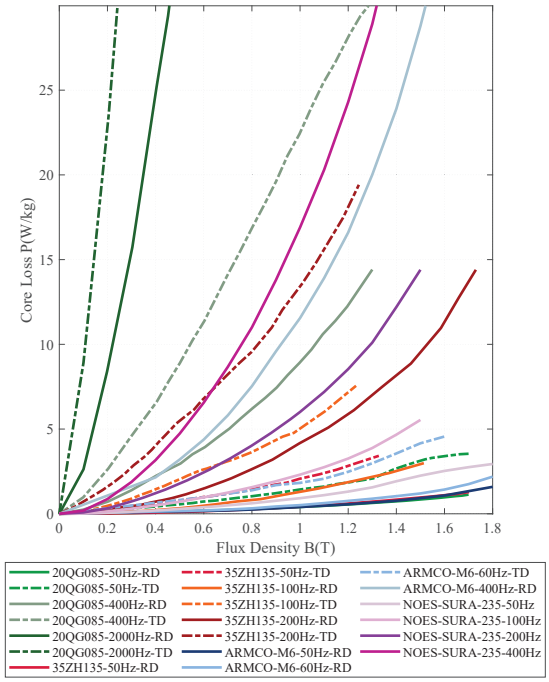


Fig. 6. *B-P* curveof selected baseline materials

GOES material, which is the focus of this work, had only RD measurements for both B-H and B-P characteristics. By analysing the directional behaviour of these base curves, the TD behaviour of the research GOES material was derived for B-P values at different frequencies in the TD, using data driven anisotropic scaling and interpolation techniques. This approach enables the reconstruction of the transverse core loss curves for a material with limited directional data.

B. Transverse BP Values for the GOES Research material

The researched GOES material loss P_{TD} was estimated using the rotational scaling factors derived from the selected base curves. Let $K_{rot}(\theta)$ denote the rotational factor relating RD and TD losses,

$$P_{TD}(B, f) = K_{rot}(\theta_{\perp}) P_{RD}(B, f) \tag{6}$$

Based on the selected base curves, the scaling factor was observed as,

$$K_{rot}(\theta) \approx \begin{cases} 1.0, & \theta \approx 0^{\circ} \\ 1.5 - 2.5, & \theta \approx 90^{\circ} \end{cases} \tag{7}$$

The TD loss values are reconstructed from the RD data using the scaling factor K_{rot} as a first-order engineering approximation of anisotropic loss behavior. A $K_{rot} = 1.65$ was selected to approximate the core loss in the TD. It can be noted that the loss coefficients in the ANSYS Maxwell software are sensitive to the B-P values. The loss coefficients K_h, K_c, K_e and the B-P data for the research material are given in the Appendix. The B-P values of the research material for varying K_{rot} are presented in Fig 7

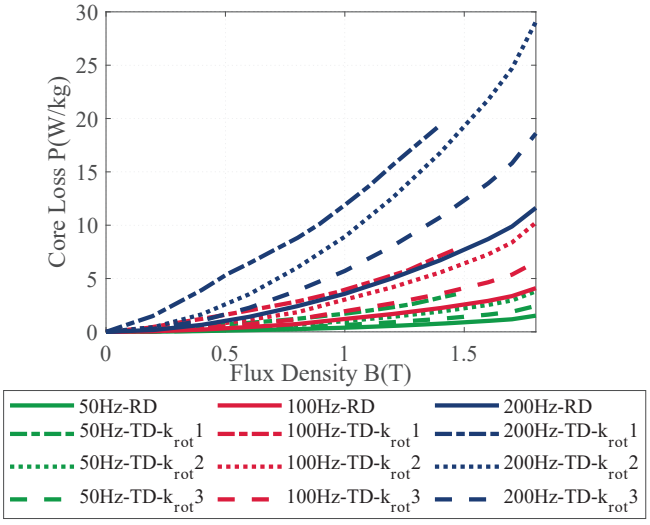


Fig. 7. *B-P* curve in RD and TD for the research GOES material at 50 Hz, 100 Hz, and 200 Hz for $K_{rot}(\theta) = \{1.0, 1.65, 2.5\}$.

VI. Core Loss Analysis with Grain-Oriented Steel

The YASA AFM was solved with GOES and NOES at rated operation. The directional dependence of core loss in the research GOES material, evaluated using $K_{rot} = 1.0, 1.65,$ and 2.5 is presented in Fig. 8. The analysis revealed that eddy current losses dominate, while hysteresis losses remain comparatively small, which is consistent with the lower loss characteristic of GOES. Scaling with $K_{rot} = 2.5$ corresponds to the extreme TD and results in an overestimation of the total losses, whereas using $K_{rot} = 1.0$ underestimates the off-axis contributions, failing to capture realistic machine operating conditions. The intermediate factor $K_{rot} = 1.65$ was selected to provide a balanced estimate of effective core loss. This approach preserves the dominance of eddy current losses, maintains low hysteresis contribution, and better reflects the material's anisotropic behaviour.

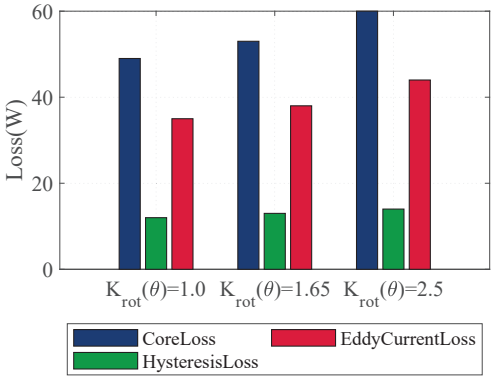


Fig. 8. Core loss, hysteresis loss, and eddy current loss comparison for varying equiavlent scaling factor at $\theta \approx 90^{\circ}$

Authorized licensed use limited to: Chalmers University of Technology Sweden. Downloaded on November 05,2026 at 14:27:58 UTC from IEEE Xplore. Restrictions apply.

The selected $K_{rot} = 1.65$ is a nominal calibrated value within the admissible range of $K_{rot}(\theta)$; the selected K_{rot} is in robust agreement with reference TD loss trends. Neighbouring values produce only marginal variation and do not alter the main conclusions.

The reconstructed TD B-P curve of the research material ($K_{rot} = 1.65$) was compared against the NOES SURA M-235-35A (with $\delta_{th} = 0.35mm$), and the two selected reference materials: Material-1 being 20QG085 (with the thinner laminations compared to all the other materials) and Material-2 being 35ZH135. The evaluated relative loss behaviour and directional scaling trends are presented in Fig. 9. The researched GOES material (with an assumed $\delta_{th} = 0.35mm$) shows a 28% reduction in the average core loss compared to the SURA M 235-35A stator core. Specifically, hysteresis loss decreased by 74%, while the eddy current loss increased by 37% relative to the SURA M 235-35A core. Furthermore, the analysis revealed the distinct characteristics across the three GOES materials. For example, in reference Material-1 the hysteresis and eddy current losses were equal ($Ph \approx Pe$). Reference Material-2 exhibited the highest total core losses compared to the research material and the first reference material. The research material produces losses between reference materials 1 and 2, providing a realistic estimate of the intermediate scaling factor used for the research material.

The reported loss reductions are interpreted as comparative trends under identical modelling assumptions rather than absolute machine-level loss predictions, since the TD behavior is reconstructed using the simplified scaling approach.

Previous comparative studies showed that the applicability of the 2D approximation depends strongly on the ratio L_m/R_{wp}. For the investigated machine, when $L_m/R_{wp} > 0.5$, the difference in predicted average core loss between the 2D and the 3D models was small, indicating that the dominant magnetic behavior is well captured in the transformed 2D plane [16]. Therefore, under this condition, the adopted 2D model provides a computationally efficient and sufficiently accurate approach for comparative core-loss evaluation, while the 3D analysis is mainly required for final validation.

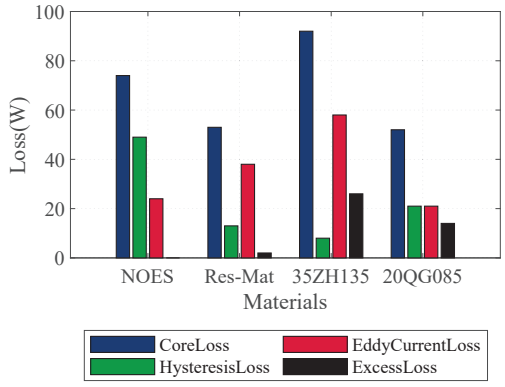


Fig. 9. Comparison of core loss, hysteresis loss, eddy current loss, and excess loss between the research material with $K_{rot} = 1.65$ and the baseline materials

VII. CONCLUSION

This work presents a practical approach for modelling the anisotropic magnetic behaviour of a research GOES using limited directional data. The B-H characteristics were divided into three flux density regions, and a piecewise scaling method was applied. The three reference materials with known RD and limited TD measurements were used. This enabled reconstruction of the TD behaviour and derivation of B-H curves for the research material.

The core loss coefficients in the TD for the research material was obtained by using the data driven scaling factor and a sensitivity analysis using scaling factors $K_{rot} = 1.0, 1.65, 2.5$. The results showed that, $K_{rot} = 2.5$ tends to overestimate the losses and $K_{rot} = 1.0$ underestimates the losses whereas, $K_{rot} = 1.65$ provides reasonable representation of loss differences between RD and TD.

The GOES material investigated was used as the stator core material in the YASA AFM. These results showed that the average core loss decreased by 28% compared to a NO stator core, with hysteresis loss reduced by 74% and eddy current loss increased by 37% relative to the NO stator core. The comparison of research material with $Krot = 1.65$ with reference materials showed the differing relationships between hysteresis and eddy current losses. Material-1, with a thinner lamination of $0.2mm$ exhibited $P_h \approx P_e$, and Material-2 and the research GOES material, both with a lamination thickness of $0.35mm$, showed dominance in eddy current loss $P_h < P_e$. Thus, the results highlight that the scaling methods must be applied carefully. Hence, the proposed framework combining B-H analysis, reference-based scaling, and sensitivity evaluation provides a practical method for estimating directional core losses of GOES. The reconstructed magnetic characteristics can therefore be used for simulation and modelling of AFMs when complete angular measurements are not available. Future work will include experimentally measured TD loss data and full directional loss modelling.

REFERENCES

[1] Farshid Mahmouditabar and Nick Baker. “A review on the effect of electrical steel manufacturing processes on the performance of electric machines”. In: *Energies* 16.24 (2023), p. 7954.

[2] Atsuhito Honda, Kunihiro Senda, and Kenichi Sadahiro. “Electrical steel for motors of electric and hybrid vehicles”. In: *Kawasaki Steel Giho* 34.2 (2002), pp. 85–89.

[3] Ji-Chang Son and Dong-Kuk Lim. “Magnetic Characteristic Analysis of Applying Grain-Oriented Electrical Steel on Traction Motors”. In: *2022 IEEE 5th Student Conference on Electric Machines and Systems (SCEMS)*. IEEE. 2022, pp. 1–4.

[4] Ji-Chang Son and Dong-Kuk Lim. “Novel stator core of the permanent magnet assisted synchronous reluctance motor for electric bicycle traction motor using grain-oriented electrical steel”. In: *2021 24th international conference on electrical machines and systems (ICEMS)*. IEEE. 2021, pp. 1215–1218.

Authorized licensed use limited to: Chalmers University of Technology Sweden. Downloaded on November 05,2026 at 14:27:58 UTC from IEEE Xplore. Restrictions apply.

[5] Yuan Cheng et al. “Influence of Stator Core Materials on Electromagnetic Performance of YASA Type Axial Flux Permanent Magnet Machines”. In: *2023 26th International Conference on Electrical Machines and Systems (ICEMS)*. IEEE. 2023, pp. 1116–1121.

[6] Cristian Demian et al. “Optimization of the tooth geometry for axial flux machine with Non-Grain Oriented and Grain Oriented electrical steel”. In: *2025 IEEE International Electric Machines & Drives Conference (IEMDC)*. IEEE. 2025, pp. 1129–1134.

[7] Weiwei Geng, Jining Hou, and Qiang Li. “Electromagnetic analysis and efficiency improvement of axial-flux permanent magnet motor with yokeless stator by using grain-oriented silicon steel”. In: *IEEE Transactions on Magnetics* 58.2 (2021), pp. 1–5.

[8] Damian Kowal et al. “Comparison of nonoriented and grain-oriented material in an axial flux permanent-magnet machine”. In: *IEEE Transactions on Magnetics* 46.2 (2010), pp. 279–285.

[9] Ravi Sundaria et al. “Effect of different cutting techniques on magnetic properties of grain oriented steel sheets and axial flux machines”. In: *IECON 2019-45th Annual Conference of the IEEE Industrial Electronics Society*. Vol. 1. IEEE. 2019, pp. 1022–1027.

[10] Armco Inc. *Armco Oriented and TRAN-COR H Electrical Steels Design Manual*. Technical Data and Design Curves. Armco Inc. Middletown, Ohio, 1986.

[11] Kyeong-Tae Yu et al. “Electromagnetic analysis and multi-objective design optimization of a WFSM with hybrid GOES-NOES core”. In: *World Electric Vehicle Journal* 16.7 (2025), p. 399.

[12] ANSYS, Inc. *Ansys Maxwell Help System, [Specific Guide/Chapter Name]*. Release 2025 R2. Accessed: March 18, 2026. ANSYS, Inc. Canonsburg, PA, 2025. URL: https://ansyshelp.ansys.com.

[13] Benjamin Ducharne et al. “An anisotropic vector hysteresis model of ferromagnetic behavior under alternating and rotational magnetic field”. In: *Journal of Magnetism and Magnetic Materials* 549 (2022), p. 169045.

[14] Vineetha Puttaraj. *Modeling of a 4kW Axial Flux Machine-Measurements and 2D/3D Modeling*. Chalmers Tekniska Hogskola (Sweden), 2025.

[15] Mikael Alatalo. *On finding optimal machines and comparison of axial and radial flux propulsion machines*. Chalmers University of Technology. Institutionen för elektroteknik, 2021.

[16] Vineetha Puttaraj, Sonja Tidblad Lundmark, and Torbjörn Thiringer. “Moving from a 3d axial flux machine model to 2d considering the impact of end leakage flux”. In: *2024 International Conference on Electrical Machines (ICEM)*. IEEE. 2024, pp. 1–7.

BIOGRAPHIES

Vineetha Puttaraj is currently a PhD student at the Division of Electrical Power Engineering within the Department of Electrical Engineering at Chalmers University of Technology, Gothenburg, Sweden, specializing in the design of electrical machines. Her research focuses on the design analysis and testing of axial flux machines for vehicle applications.

Sonja Tidblad Lundmark received her M.Sc. (Eng.) and Ph.D. degrees from Chalmers University of Technology, Gothenburg, Sweden, in 1992 and 2005, respectively. Since July 2013, she has been an Associate Professor at the Division of Electric Power Engineering at Chalmers University of Technology. Her research interests are in the areas of electrical machines and drives.

Torbjörn Thiringer works at Chalmers University of Technology, in Göteborg Sweden, as a professor in applied power electronics. He took his M.Sc and Ph.D at Chalmers University of Technology in 1989 and 1996 respectively. His areas of interest include the modeling, control and grid integration of wind energy converters into power grids, battery technology from detailed cell modelling to system aspects, as well as power electronics and drives for other types of applications, such as electrified vehicles, buildings and industrial applications.

APPENDIX A
RESEARCH MATERIAL DATA

A. B-H curve Data

Rolling Direction		Transverse Direction	
H (A/m)	B (T)	H (A/m)	B (T)
0	0	0	0
10	0.4	20	0.4
20	1	50	1
50	1.5	150	1.1
100	1.8	300	1.3
500	1.9	500	1.4
1000	1.93	800	1.42
5000	2	1500	1.45
10000	2.05	3000	1.5
		5000	1.53
		7000	1.6
		9000	1.66
		10000	1.7

B. B-P curve data

B(T)	Rolling Direction P (W/kg)			Transverse Direction P (W/kg)		
	50 Hz	100 Hz	200 Hz	50 Hz	100 Hz	200Hz
0	0	0	0	0	0	0
0.2	0.017	0.055	0.178	0.03	0.088	0.285
0.4	0.067	0.211	0.655	0.11	0.338	1.048
0.6	0.15	0.452	1.414	0.24	0.723	2.262
0.8	0.259	0.733	2.405	0.41	1.173	3.848
1	0.402	1.21	3.57	0.64	1.936	5.712
1.2	0.565	1.674	5.03	0.9	2.678	8.048
1.4	0.761	2.23	6.72	1.22	3.568	10.752
1.6	1.01	2.905	8.7	1.62	4.648	13.92
1.7	1.18	3.353	9.88	1.89	5.365	15.808
1.8	1.52	4.098	11.63	2.43	6.557	18.608

C. Boundary and Loss-coefficient data

Parameter	Value
B_1	1.0 T
B_2	1.53 T
H_1	50 A/m
H_2	5000 A/m
n	3
$K_h(RD)$	45.041
$K_c(RD)$	0.434
$K_e(RD)$	0.4611
$K_h(TD)$	72.074
$K_c(TD)$	0.694
$K_e(TD)$	0.737
mass density	7850 kg/m^3

Authorized licensed use limited to: Chalmers University of Technology Sweden. Downloaded on November 05,2026 at 14:27:58 UTC from IEEE Xplore. Restrictions apply.